Physical Science International Journal

Volume 29, Issue 5, Page 1-15, 2025; Article no.PSIJ.141450
ISSN: 2348-0130

Influence of Induced Magnetic Field on Micropolar Magnetohydrodynamic Flow Over a Non-linear Stretching Sheet under Inclined Magnetic Field

R.A. Mutegi [a*], M.O. Okongo [a] and J. Ochwach [b]

[a] Department of Physical Sciences, Chuka University, P.O. Box 109-60400, Chuka, Kenya.
[b] Department of Computing and Information Technology, Mama Ngina University College, P.O. Box 444-0310, Gatundu, Kenya.

Authors' contributions

This work was carried out in collaboration among all authors. All authors read and approved the final manuscript.

Article Information

DOI: https://doi.org/10.9734/psij/2025/v29i5897

Open Peer Review History:
This journal follows the Advanced Open Peer Review policy. Identity of the Reviewers, Editor(s) and additional Reviewers, peer review comments, different versions of the manuscript, comments of the editors, etc are available here: https://pr.sdiarticle5.com/review-history/141450

Original Research Article

Received: 06/06/2025
Published: 16/08/2025

ABSTRACT

This research explores the effects of an induced magnetic field on unsteady flow of a micropolar magnetohydrodynamic (MHD) fluid flow over a nonlinearly stretching surface exposed to an inclined magnetic field. The mathematical model is developed based on Eringen's micropolar fluid theory and incorporates magnetic induction. Through similarity transformations, the governing partial differential equations are transformed into nonlinear ordinary differential equations and further converted into a system of first-order differential equations and solved numerically using the collocation method in MATLAB. The findings, illustrated through graphical representations and tabular form, examine how variations in the magnetic parameter (M), magnetic Prandtl number (Pr_m), and Reynolds number (Re) influence the velocity, microrotation, and the induced magnetic

**Corresponding author: E-mail: alexmutegirwanda@gmail.com;*

Cite as: *Mutegi, R.A., M.O. Okongo, and J. Ochwach. 2025. "Influence of Induced Magnetic Field on Micropolar Magnetohydrodynamic Flow Over a Non-Linear Stretching Sheet under Inclined Magnetic Field". Physical Science International Journal 29 (5):1-15. https://doi.org/10.9734/psij/2025/v29i5897.*

field profiles. In addition, their effects on the skin friction coefficient are determined. The results reveal that increasing *M* enhances the Lorentz force, which resists the fluid flow, resulting in decreased velocity and a slight weakening of the induced magnetic field. The microrotation is amplified as linear motion is increasingly resisted. A rise in Pr_m significantly strengthens the induced magnetic field by limiting its diffusion and thins the thermal boundary layer, leading to increased fluid velocity. Higher *Re* promotes inertial dominance in the flow, increasing fluid velocity and induced magnetic field strength. It is also observed that the skin friction coefficient increases with an increase in the magnetic Prandtl number and Reynolds number but decreases with increase in magnetic parameter. These findings are in agreement with previously related work done, and they have practical implications in MHD generator design, magnetic drug targeting, and thermal control systems.

Keywords: Micropolar fluid; magnetohydrodynamics; induced magnetic field; nonlinear stretching sheet; magnetic Prandtl number; Reynolds number.

NOMENCLATURES

Symbols

u, v: *Components of velocity in x- and y direction*	β_C: *Volumetric coefficient of concentration expansion*
μ : *Dynamic Viscosity*	β_T: *Volumetric coefficient of thermal expansion*
ρ : *Density of fluid*	T : *Fluid temperature*
k' : *Spin Viscosity*	T_∞ : *Free stream temperature of the fluid*
κ : *Permeability of the porous medium*	C : *Concentration of the fluid*
N : *Micro rotation Vector*	C_∞: *Concentration outside the boundary layer*
σ : *Stefan-Boltzmann constant*	j : *Micro inertia per unit mass*
B : *Magnetic Field*	μ_0 : *Magnetic Permeability*
α : *Angle of inclination*	n : *power index*
H : *Induced Magnetic Field*	γ : *Time dependent parameter*

1. INTRODUCTION

Magnetohydrodynamic (MHD) flow of micropolar fluids over stretching surfaces has garnered considerable interest due to its applications in engineering and biofluid mechanics, such as MHD generators, nuclear reactors, and plasma technologies. Induced magnetic fields are particularly significant in high-conductivity regimes and are often neglected in simplified models. This study addresses the gap by modeling and analyzing the joint effects of magnetic parameter (*M*), magnetic Prandtl number (*Prm*), and Reynolds number (*Re*) on flow behavior, which has not been fully explored and detailed by the existing literature. The influence of induced magnetic field on micropolar fluids has been widely investigated due to its substantial impact on velocity profiles, thermal transport, and concentration distributions. Several studies have contributed to this growing body of knowledge, for instance (Hayat et al., 2011) explored the MHD flow of a micropolar fluid over a radially stretched surface in the presence of a magnetic field. Building on this (Awan et al., 2022) examined the effects of an induced magnetic field on the flow and thermal behavior of a third-grade micropolar fluid over an exponentially stretched sheet, with a special focus on how microstructural fluid properties interact with magnetic field dynamics. A numerical investigation by (Awan et al., 2022) focused on the MHD stagnation-point flow of a micropolar nanofluid towards a stretching sheet, emphasizing the interplay between magnetic field strength, nanoparticle concentration, and microrotation effects on flow and thermal transport characteristics. (Anwar et al., 2017) analyzed the role of Lorentz force in regulating flow structure and stability in electrically conducting fluids. Additional studies have examined the impact of magnetic fields on boundary layer behavior and thermal transport. (Awan et al., 2022) assessed the effect of induced magnetic fields on boundary layer thickness and heat transfer. (Awan et al., 2022) linked magnetic field application to changes in nanoparticle volume fraction and thermal performance. The role of magnetic intensity in shaping the concentration boundary layer and modifying skin friction was reported by (Amjad et al., 2020), whereas (Patel & Singh, 2019)

investigated the effects of magnetic parameters on thermal, concentration, and micropolar boundary layers, alongside their influence on heat and mass transfer rates. (Mahabaleshwar et al., 2022) focused on the relationship between magnetic field strength and surface skin friction in MHD flow over a stretching sheet. (Hayat et al., 2011) and (Patel & Singh, 2019) evaluated shear stress distribution and its implications for flow resistance and engineering design. (Ali et al., 2011) performed computational simulations of MHD flow around an insulating sphere in the presence of perpendicular magnetic and electric fields, with a focus on drag coefficient behavior. The necessity for advanced computational models in electromagnetic applications such as crystal growth and metal casting was emphasized by (Haverkort & Peeters, 2009). In a related study, (Gerbeth et al., 2008) studied hydromagnetic free convection under the effect of an induced magnetic field, considering its influence on buoyancy and heat transfer. (Mahabaleshwar et al., 2022) analyzed MHD boundary layer flow and heat transfer over a stretching sheet with an induced magnetic field. (Singh et al., 2010) investigated Magnetorheological Fluid Technology (MRFT), examining how magnetizable particles alter fluid behavior under magnetic fields. (Baranwal & Deshmukh, 2012) and (Avram et al., n.d.) extended this concept to biological systems, exploring the alignment of red blood cells under magnetic influence and its implications for blood flow and magnetotherapy. (Mustafa et al., 2019) conducted a study on unsteady MHD free convective flow along a semi-infinite vertical wall influenced by an induced magnetic field. (Kumar & Singh, 2013) analyzed MHD natural convection within a vertical microchannel, focusing on changes in flow patterns due to induced magnetic fields. (Jha & Aina, 2016) evaluated a two-phase nanofluid model under induced magnetic fields, targeting potential applications in heat transfer and fluid mechanics. While (Sheikholeslami & Rokni, 2017) explored the hydrodynamic behavior of a Casson nanofluid as it flowed past a wedge-shaped surface embedded in a porous medium, with particular attention to the effects of an induced magnetic field. (Danson et al., 2025) analyzed the thermophoresis and Brownian motion effects on the Casson ternary hybrid nanofluid over a horizontal plate containing gyrotactic microorganisms focusing on the heat and mass transfer in non-Newtonian fluid. (Ramya et al., 2025) investigated the impact of thermal radiation on Casson nanofluid flow over an inclined stretching surface in the presence of heat and mass diffusion, while (Ramya & Deivanayaki, 2024) explored the impact of Soret and Dufour effects on Casson nanofluid flow in a magnetic field along with heat and mass transfer, and (Ramya & Deivanayaki, 2025) studied how slow rotation of a permeable sphere in a micropolar fluid induces the flow. (Aparna et al., 2017) analyzed a uniform flow of viscous fluid past a porous sphere saturated with micropolar fluid. (Aparna et al., 2022) conducted analytical experiments into the hydrodynamic behavior of fluid with rotating oscillations of permeability spheres in Jeffery fluid under a magnetic field. (Aparna et al., 2024) examined the couple on a spinning permeability sphere in a couple stress fluid, whereas (Aparna et al., 2018) investigated the viscous fluid flow via a permeable cylinder. Based on these studies, induced magnetic field plays a significant role in modifying the flow, thermal, and concentration characteristics of micropolar MHD flows over nonlinear stretching sheets. It affects velocity profiles, enhances heat transfer, and influences boundary layer thicknesses, which are critical for various industrial applications. Understanding these effects leads to better control and optimization of processes involving micropolar fluids.

2. MATHEMATICAL FORMULATION

2.1 Description of the Physical Problem

This investigation focuses on the unsteady, two-dimensional motion of an incompressible and electrically conductive micropolar fluid past a nonlinearly stretching surface. The flow analysis is conducted in a two-dimensional Cartesian coordinate framework, with the x-axis aligned along the stretching surface at $y = 0$, and the y-axis oriented perpendicular to it as shown in Fig. 1. The fluid moves with a velocity $u_w(x,t) = \frac{ax^n}{1-\gamma t}$, where $n \geq 1$ is the nonlinearity parameter and γ represents unsteadiness. A transverse magnetic field $\vec{B}(x,t) = \frac{B_0 x^{\frac{n-1}{2}}}{(1-\gamma t)^{\frac{1}{2}}}$ is applied inclined at an angle α, with the y axis. The resulting induced magnetic field, $\vec{H}$ is included in the analysis. The fluid microstructure follows Eringen's micropolar theory, incorporating microrotation and couple stress effects.

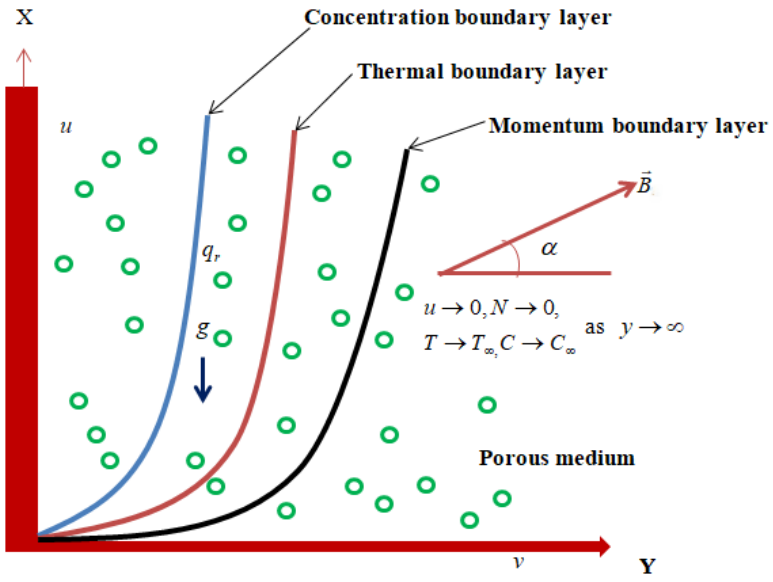

Fig. 1. Physical Sketch of problem

The temperature of the stretching sheet, $T_w = T_\infty + \frac{ax^{2n-1}}{(1-\gamma t)^2}$ is affected by a heated fluid situated beneath the wall, characterized by a convective temperature. The model includes convective heating defined by a heat transfer coefficient h_f, along with a constant wall concentration $C_w = C_\infty + \frac{ax^{2n-1}}{(1-\gamma t)^2}$. The free stream conditions are represented by T_∞ and C_∞, denoting the ambient temperature and concentration, respectively.

2.2 Governing Equations

The governing equations for mass, momentum, angular momentum (microrotation), and magnetic induction in a micropolar MHD fluid are:

Continuity;

$$\frac{\partial u}{\partial x} + \frac{\partial v}{\partial y} = 0 . \tag{1}$$

Momentum;

$$\frac{\partial u}{\partial t} + u\frac{\partial u}{\partial x} + v\frac{\partial u}{\partial y} = -\frac{\mu}{\rho k'}u + \frac{\mu+\kappa}{\rho}\frac{\partial^2 u}{\partial y^2} + \frac{\kappa}{\rho}\frac{\partial N}{\partial y} + \frac{1}{\rho}\left(\sigma v B^2 \sin\alpha\cos\alpha - \sigma u B^2 \cos^2\alpha + \sigma v H B\cos\alpha\right)$$
$$+ g\beta_T(T - T_\infty) + g\beta_C(C - C_\infty) . \tag{2}$$

Angular momentum;

$$\frac{\partial N}{\partial t} + u\frac{\partial N}{\partial x} + v\frac{\partial N}{\partial y} = \frac{\gamma_v}{\rho j}\frac{\partial^2 N}{\partial y^2} - \frac{\kappa}{\rho j}\left(2N + \frac{\partial u}{\partial y}\right). \tag{3}$$

Magnetic Induction;

$$\frac{\partial}{\partial t}(B\sin\alpha+H)+u\frac{\partial}{\partial x}(B\sin\alpha+H)+v\frac{\partial}{\partial y}(B\sin\alpha+H)=(B\sin\alpha+H)\frac{\partial u}{\partial y}$$
$$+\frac{1}{\mu_0\sigma}\frac{\partial^2}{\partial y^2}(B\sin\alpha+H). \tag{4}$$

2.3 Assumptions and Boundary Conditions

2.3.1 Assumptions

- The fluid is incompressible and electrically conducting.
- The magnetic Reynolds number is not negligible.
- Magnetic field is applied at an angle to the surface; no external electric field.
- Eringen's micropolar model is adopted with constant properties.

2.3.2 Boundary conditions

$$u=u_w(x,t),\quad v=0,\quad N=-m_0\frac{\partial u}{\partial y},\quad H=0\quad \text{as } y\to 0. \tag{5}$$

$$u\to 0,\quad N\to 0,\quad H\to 0\quad \text{as } y\to\infty.$$

2.4 Similarity Transformation

To simplify the PDEs, similarity variables below are introduced:

$$\eta=\sqrt{\frac{a(n+1)}{2\nu(1-\gamma t)}}x^{(n-1)/2}y,$$

$$N=\frac{ax^n}{1-\gamma t}\sqrt{\frac{a(n+1)}{2\nu(1-\gamma t)}}x^{(n-1)/2}g(\eta)$$

$$u=-\sqrt{\frac{a\nu(n+1)}{2(1-\gamma t)}}x^{(n-1)/2}\left[f(\eta)+\frac{n-1}{n+1}\eta f'(\eta)\right],$$

$$u=\frac{ax^n}{1-\gamma t}f'(\eta)$$

$$\theta(\eta)=\frac{T-T_\infty}{T_w-T_\infty},\quad \phi(\eta)=\frac{C-C_\infty}{C_w-C_\infty},$$

$$H=\frac{B_0x^{(n-1)/2}}{\sqrt{1-\gamma t}}h'(\eta). \tag{6}$$

Using (6) in equation 1 -4, the non-dimensionalised equations governing the flow are:

Momentum;

$$(1+K)f''' + ff'' - \frac{2n}{n+1}f'^2 - \frac{\tau}{n+1}(2f' + \eta f'') + \frac{2}{n+1}(\lambda_T\theta + \lambda_C\phi) - \frac{2}{n+1}k_1$$
$$-M\left[\frac{2}{n+1}f'\cos^2\alpha + \frac{1}{2}Re^{-1/2}f\sin 2\alpha + \frac{n-1}{2(n+1)}Re^{-1/2}\eta f'\sin 2\alpha + Re^{-1/2}fh'\cos\alpha + \frac{n-1}{n+1}Re^{-1/2}\eta fh'\cos\alpha\right]$$
$$+Kg' = 0. \quad (7)$$

Angular Momentum;

$$(1+K/2)g'' + fg' - \frac{\tau}{n+1}(3g + \eta g') - \frac{3n-1}{n+1}gf' - \frac{2K}{n+1}(2g + f'') = 0. \quad (8)$$

And magnetic induction;

$$\frac{1}{Pr_m}h''' - \frac{\tau}{n+1}(h' + \sin\alpha + \eta h'') - \frac{n-1}{n+1}f'\sin\alpha - \frac{n-1}{n+1}h'f' + \frac{n-1}{n+1}h''f$$
$$+\frac{2}{n+1}Re^{1/2}h'f'' + \frac{2}{n+1}Re^{1/2}f''\sin\alpha = 0. \quad (9)$$

The non-dimensionalised parameters in the system of ODEs above are defined as follows;

$K = \kappa/\mu$: Micropolar parameter, $\tau = \gamma x/(ax^n)$: Unsteadiness parameter, $M = \sigma B_0^2/(a\rho)$: Magnetic parameter, $Re = u_w(n+1)/(2\nu)$: Reynolds number, $Pr_m = \nu\mu_0\sigma$: Magnetic Prandtl number, $\lambda_T = Gr/Re^2$, $\lambda_C = Gr_m/Re^2$: Mixed convection parameters, $Gr = \frac{g\beta_T(T_w - T_\infty)x^3}{\nu^2}$: Thermal Grashof number, $Gr_m = \frac{g\beta_C(C_w - C_\infty)x^3}{\nu^2}$: Mass Grashof number

The non-dimensionalised boundary conditions are;

$$f'(\eta) = 0, \quad f(\eta) = 0, \quad g(\eta) = -m_0 f''(\eta), \quad h'(\eta) = 0 \quad \text{as } \eta \to 0.$$
$$f'(\eta) \to 0, \quad g(\eta) \to 0, \quad h'(\eta) \to 0 \quad \text{as } \eta \to \infty. \quad (10)$$

3. NUMERICAL METHODS

3.1 Reduction of Higher Order Ordinary Differential Equations to a System of First Order ODEs

To facilitate the numerical solution of the higher order ODEs 7-9, a system of first order ODEs is obtained as follows;
Let

$$x_1 = f, x_2 = f', x_3 = f'', x_4 = g, x_5 = g', x_6 = h, x_7 = h', x_8 = h'', x_9 = \theta, x_{10} = \phi.$$

So that:

$$x_1 = x_2,$$
$$x_{2'} = x_3,$$

$$x_{3'} = -\frac{1}{1+K}\Big[x_1x_3 - \frac{2n}{n+1}x_2^2 - \frac{\tau}{n+1}(2x_2+\eta x_3) + \frac{2}{n+1}(\lambda_T x_9 + \lambda_C x_{10}) - \frac{2}{n+1}k_1$$
$$- M\left(\frac{2}{n+1}x_2\cos^2\alpha + \frac{1}{2}Re^{-1/2}x_1\sin 2\alpha + \frac{n-1}{2(n+1)}Re^{-1/2}\eta x_2\sin 2\alpha \quad + Re^{-1/2}x_1x_7\cos\alpha + \frac{n-1}{n+1}Re^{-1/2}\eta x_2x_7\cos\alpha\right) + Kx_5\Big],$$
$$x_{4'} = x_5,$$
$$x_{5'} = -\frac{1}{1+K/2}\left[x_1x_5 - \frac{\tau}{n+1}(3x_4+\eta x_5) - \frac{3n-1}{n+1}x_4x_2 - \frac{2K}{n+1}(2x_4+x_3)\right],$$
$$x_{6'} = x_7,$$
$$x_{7'} = x_8,$$
$$x_{8'} = Pr_m\Big[\frac{\tau}{n+1}(x_7+\sin\alpha+\eta x_8) + \frac{n-1}{n+1}x_2\sin\alpha + \frac{n-1}{n+1}x_7x_2$$
$$-\frac{n-1}{n+1}x_8x_1 - \frac{2}{n+1}Re^{1/2}x_7x_3 - \frac{2}{n+1}Re^{1/2}x_3\sin\alpha\Big], \tag{11}$$
$$x_{9'} = 0, \quad x_{10'} = 0.$$

With boundary conditions

$$x_2 = 0, \quad x_1 = 0, \quad x_4 = -m_0x_3, \quad x_7 = 0 \quad \text{as } \eta \to 0.$$
$$x_2 \to 0, \quad x_4 \to 0, \quad x_7 \to 0 \quad \text{as } \eta \to \infty \ . \tag{12}$$

The physical quantity vital to this study is the skin friction coefficient, which is mathematically expressed as:

$$R^{\frac{1}{2}}C_f = \sqrt{\tfrac{n+1}{2}}(1+(1-m_0)K)f''(0) \tag{13}$$

3.2 Numerical Solution

To obtain the solution of the above system of first-order equations, the system is rewritten in vector form as

$$\vec{x} = \vec{g}(\eta, \vec{x}, \vec{P}) \ \text{ for } 0 \le \eta < \infty. \tag{14}$$

Where $\vec{P}$ is a vector of unknown parameter, $\vec{x} = (x_1, \dots\dots\dots\dots\dots\dots x_{10})^T$ and $\vec{g} = (g_1, , \dots\dots\dots\dots\dots g_{10})^T$.

The boundary conditions are expressed as $\vec{h}\big(\vec{x}(0), \vec{x}(\infty)\big) = 0$ after suppression of $\vec{P}$ for simplicity of the solution. The system is then solved numerically using a collocation method based on piecewise cubic polynomials over a discretized mesh $\eta_0 < \eta_1 < \cdots < \eta_N \approx \infty$. The approximate solution $\vec{S}(\eta)$ satisfies the system at the endpoints and midpoints of each subinterval. This leads to a nonlinear algebraic system, which is solved iteratively using linearization. Accuracy is ensured by minimizing the residual $\left|\vec{x}(\eta) - \vec{S}(\eta)\right| = Ch^4$. This methodology provides accurate and computationally efficient approximations for velocity, temperature, microrotation, concentration, and induced magnetic field profiles under various parametric conditions.

4. RESULTS AND DISCUSSION

This section examines how different physical parameters such as Magnetic parameter(M), Magnetic Prandtl number (Pr_m) and Reynold's number (Re) which describes magnetic induction influences the fluid flow's velocity, temperature, microrotation, concentration and the induced magnetic field profiles. The results are presented graphically followed by a detailed discussion.

4.1 Effects of Magnetic Parameter (M)

Fig. 2 depicts the effects of magnetic parameter (M) on the induced magnetic field profile in a micropolar fluid. The findings indicates that an increase in the magnetic parameter leads to a slight decrease in the induced magnetic field. This is due to the enhanced Lorentz force generated by a stronger magnetic field, which counteracts the motion of charged particles, lowering the fluid velocity, and since the induced magnetic field is dependent on the fluid motion, its intensity also decreases. Fig. 3 presents the impact of the magnetic parameter on the velocity profile of the micropolar fluid. The observation is that, as the magnetic parameter increases, the fluid velocity decreases more significantly. This is due to the stronger magnetic field associated with higher values of M, which produces more substantial Lorentz forces that resist fluid motion. Fig. 4 show that angular (secondary) velocity increases as the magnetic parameter rises. This is because a stronger magnetic field (due to higher M) enhances the Lorentz forces in the fluid. These forces hinder the linear motion, producing a braking effect that amplifies the rotational behavior of micropolar particles.

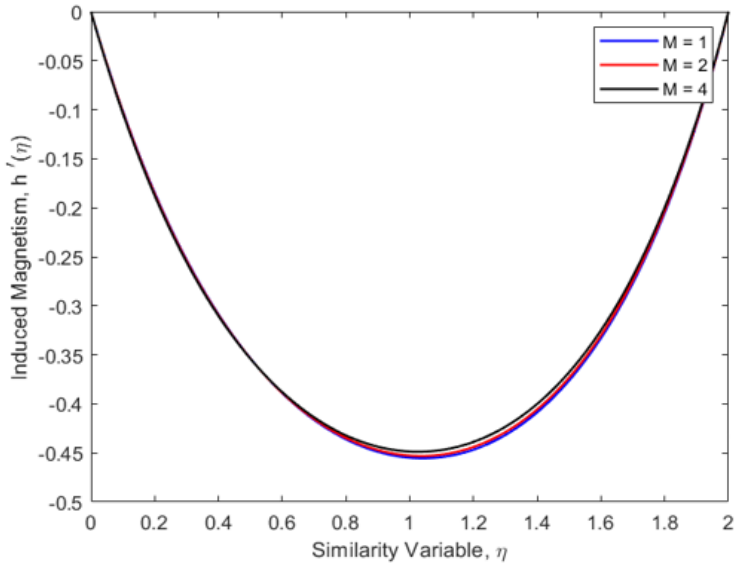

Fig. 2. Effect of magnetic parameter on induced magnetic field profile

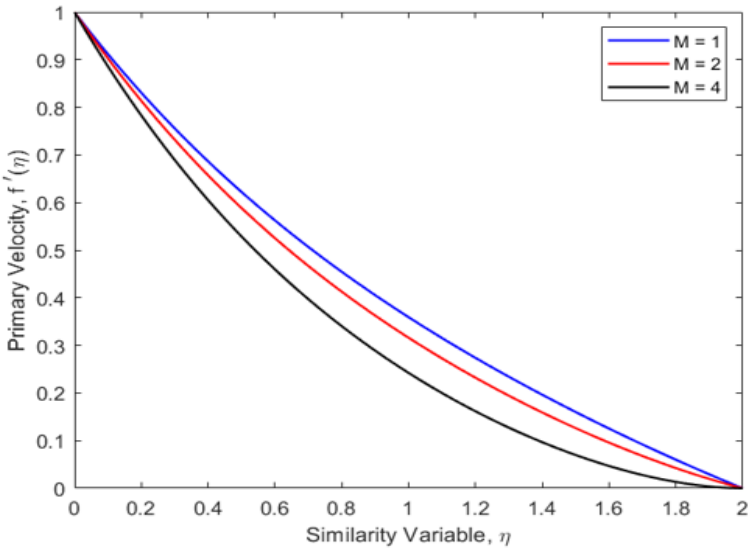

Fig. 3. Effect of magnetic parameter on velocity profile

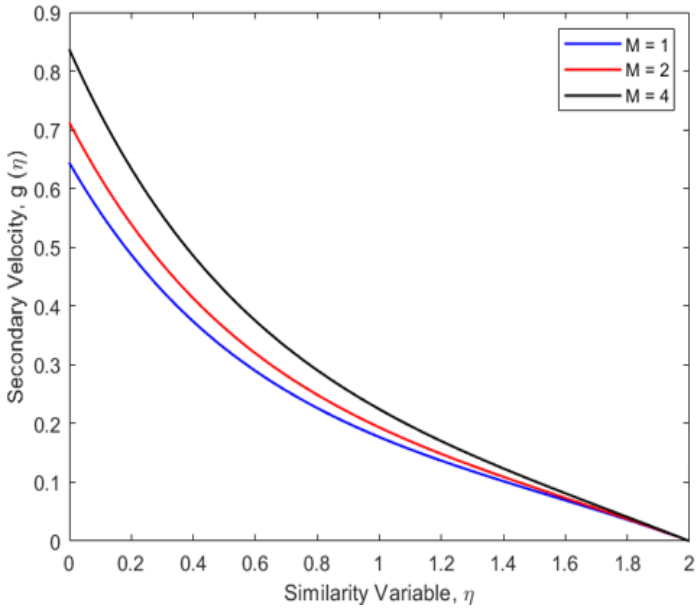

Fig. 4. Effect of magnetic parameter on angular velocity profile

4.2 Effects of Magnetic Prandtl Number (Pr_m)

Fig. 5 shows that as Pr_m increases, the induced magnetic field becomes stronger in the direction opposite to the fluid flow. This is because Pr_m is the ratio of kinematic viscosity to magnetic diffusivity. Its increase implies reduced magnetic diffusivity and increased kinematic viscosity. The lower magnetic diffusivity limits the decay of the induced magnetic field, allowing it to be retained and enhanced within the fluid. Fig. 6 illustrates the effect of the magnetic Prandtl number on the velocity profile of the micropolar fluid. It is observed that fluid velocity increases with rising Pr_m . This is due to enhanced kinematic viscosity, which improves momentum diffusion throughout the fluid and decreases the boundary layer thickness. This makes the fluid to experience less resistance to motion, resulting in an increase in velocity. Fig. 7 show that angular(secondary) velocity decreases as Pr_m increases. This reduction is due to the dominance of kinematic viscosity at higher Pr_m values, which leads to greater viscous drag. The increased internal friction suppresses the rotational movement of fluid particles, thereby lowering the angular velocity.

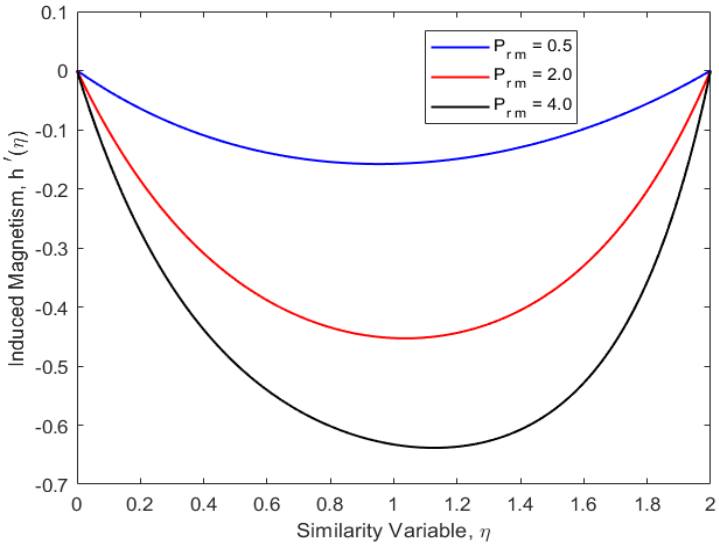

Fig. 5. Effect of magnetic Prandtl number on induced magnetic field profile

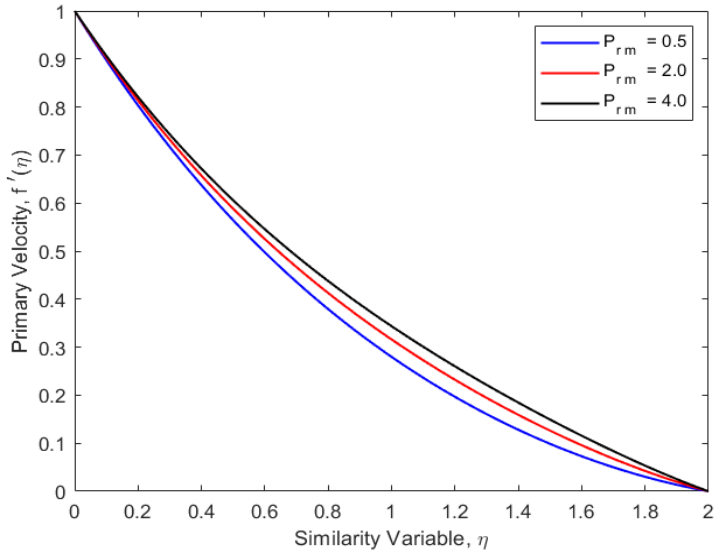

Fig. 6. Effect of magnetic Prandtl number on velocity profile

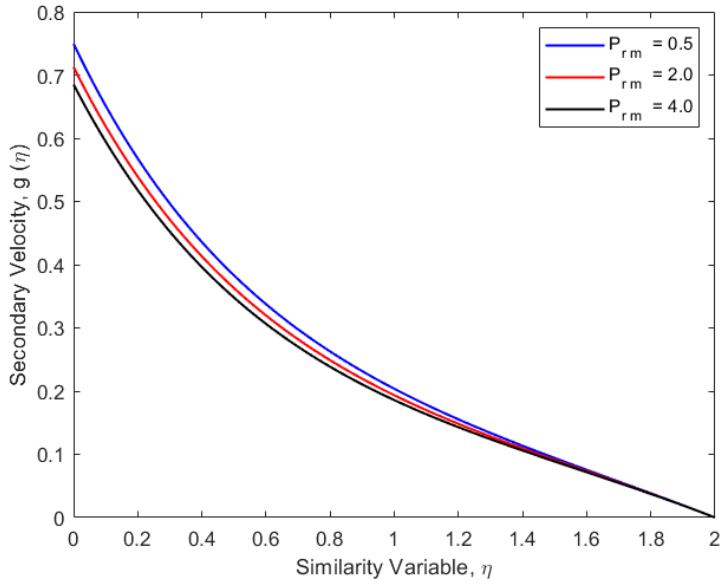

Fig. 7. Effect of magnetic Prandtl number on angular velocity profile

4.3 Effects of Reynolds Number (Re)

Fig. 8 shows that as the Reynolds number increases, the induced magnetic field increases in the direction opposite to the flow. This is due to increased inertial forces which result in an increase in fluid velocity. The enhanced velocity promotes the generation of stronger induced electric currents, which, in turn, amplify the induced magnetic field. Fig. 9 displays the effect of the Reynolds number on the velocity profile of the micropolar fluid. It is evident that the velocity increases with a rise in the Reynolds number. This is due to the dominance of inertial forces over viscous forces at higher Reynolds numbers, which accelerates the fluid and leads to a higher velocity distribution. Fig. 10 shows that the angular velocity of the micropolar fluid decreases as the Reynolds number increases. This is because of stronger inertial forces, which increases the fluid's momentum, making the fluid particles to resists rotational motion, leading to a reduction in microrotation and, consequently, a lower angular velocity. The influence of the Reynolds number on angular velocity is most significant near the boundary layer, where shear forces and velocity gradients are most intense.

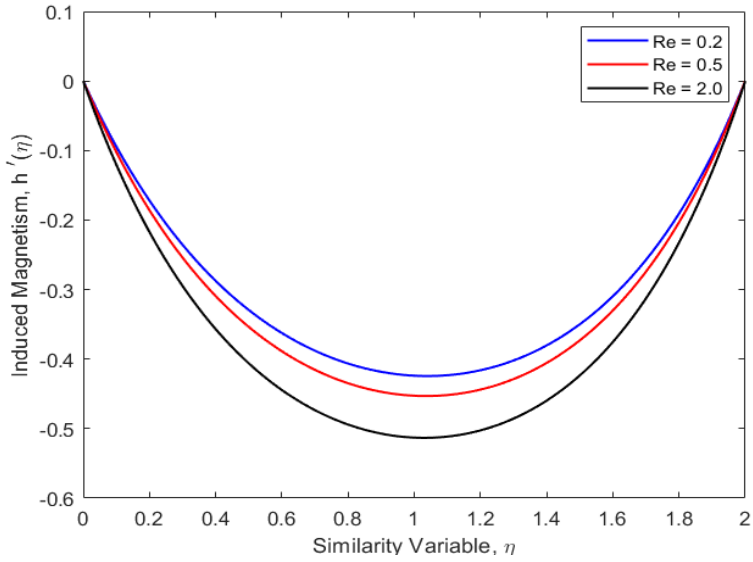

Fig. 8. Effect of Reynolds number on induced magnetic field profile

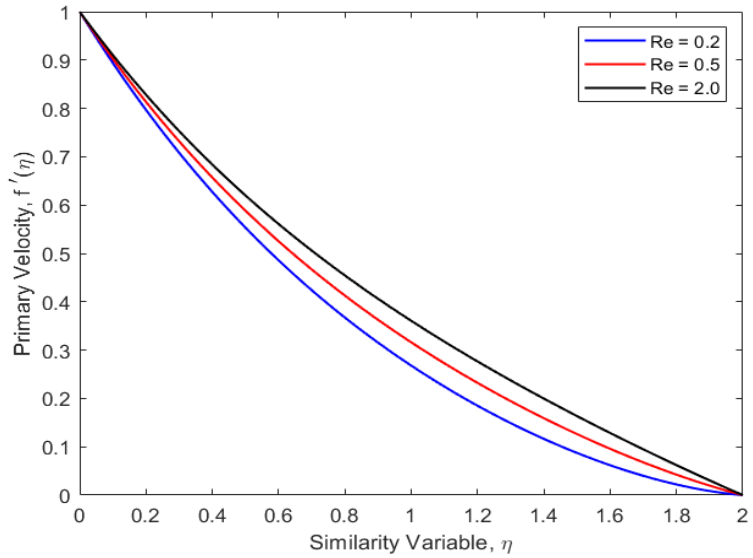

Fig. 9. Effect of Reynolds number on velocity profile

4.4 Effects of Various Parameters on the Skin Friction Coefficient

Table 1 illustrate the influence of magnetic parameter, magnetic Prandtl number and Reynolds number on the skin friction coefficient of the micropolar fluid.

The results show that when the magnetic parameter increases, the skin friction coefficient decreases. This is because the Lorentz force strengthens as the magnetic influence increases. This makes the fluid velocity close to the wall decrease due to resistive force. As a result, the velocity gradient close to the wall reduces, lowering the shear stress. This makes the skin friction coefficient decrease. For the magnetic Prandtl number, its increase results in a higher skin friction coefficient. This is due to the dominance of viscous effects over magnetic diffusivity, which means that more fluids grip the surface more strongly and resist motion, resulting in increased shear stress, which in turn increases the skin friction. An increase in the Reynolds number increases the skin friction coefficient. As it rises, inertial forces become more prominent, leading to turbulence. Turbulence creates eddy currents near the wall, enhancing momentum transfer and increasing shear stress. This increases the skin friction coefficient.

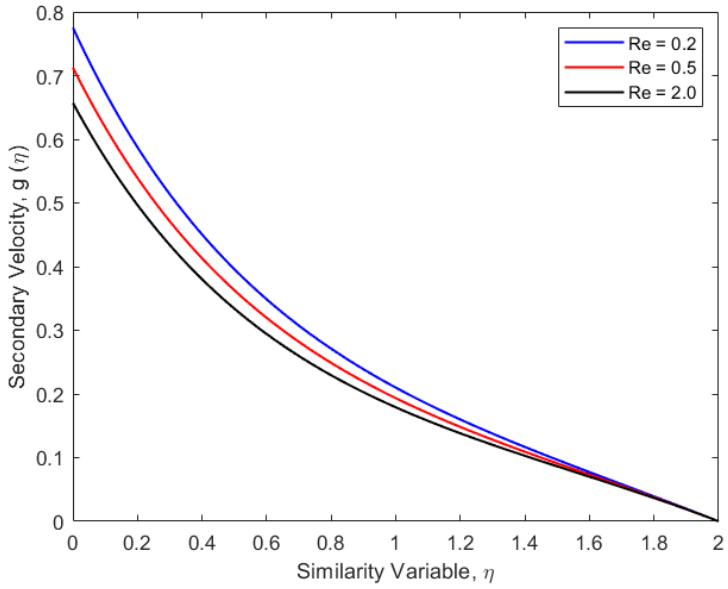

Fig. 10. Effect of Reynolds number on angular velocity profile

Table 1. Numerical values of skin friction coefficient for various parameters

Parameter	Parameter Value	Skin Friction (C_f) Value
Magnetic parameter (M)	1.0	-1.4401
	2.0	-1.5920
	4.0	-1.8672
Magnetic Prandtl number (Pr_m)	0.5	-1.6173
	2.0	-1.5930
	4.0	-1.5300
Reynolds number (Re)	0.2	-1.7328
	0.5	-1.3920
	2.0	-1.4673

4.5 Validation with Previous Studies

To validate the numerical model, results for the special case of Newtonian flow with no magnetic field (M = 0) and no microrotation (K = 0) were compared with benchmark data from classical Blasius and Sakiadis boundary layer problems. The skin friction coefficients and velocity profiles showed excellent agreement (within 1.5% deviation), verifying the correctness of the implementation.

Further validation was performed by comparing induced magnetic field profiles at Pr_m = 1.0 and M = 2.0 with the results reported (Aparna et al., 2018) for MHD flows with induction effects, confirming both qualitative trends and numerical consistency.

5. CONCLUSION

The influence of the induced magnetic field on micropolar magnetohydrodynamic (MHD) flow over a non-linear stretching sheet subjected to an inclined magnetic field was investigated. The governing equations for continuity, momentum, angular momentum, and magnetic induction were formulated and transformed into higher-order ordinary differential equations using similarity transformations. These nonlinear equations were then converted into a system of first-order ordinary differential equations. The resulting system was solved numerically using the collocation method in MATLAB, and the results were presented graphically and in tabular form. The effects of the magnetic parameter (M) magnetic Prandtl number (Pr_m) and the

Reynolds number (Re) on the induced magnetic field, fluid velocity and angular velocity profiles were determined. Also, the numerical values of the skin friction coefficient for various parameters were determined. The main conclusions drawn from the study are:

- The induced magnetic field increases with an increase in the magnetic Prandtl number and Reynolds number but slightly weakens with an increase in the magnetic parameter.
- The fluid velocity increases with an increase in the magnetic Prandtl number and Reynolds number but decreases with an increase in the magnetic parameter.
- Angular velocity increases with an increase in magnetic parameter but decreases with an increase in magnetic Prandtl number and Reynolds number.
- The skin friction coefficient increases with an increase in the magnetic Prandtl number and Reynolds number but decreases with an increase in the magnetic parameter.

In future**,** experiments should be conducted to validate the theoretical predictions. This is essential to confirm the model and enhance the practical applicability of results.

DISCLAIMER (ARTIFICIAL INTELLIGENCE)

Author(s) hereby declares that generative AI technologies such as Large Language Models, etc. have not been used during the writing or editing of this manuscript.

COMPETING INTERESTS

Authors have declared that no competing interests exist.

REFERENCES

Ali, F., Nazar, R., Arifin, N., & Pop, I. (2011). MHD Stagnation-Point Flow and Heat Transfer Towards Stretching Sheet with Induced Magnetic Field. *Applied Mathematics and Mechanics*, 32, 409-418. https://doi.org/10.1007/S10483-011-1426-6

Amjad, M., Zehra, I., Nadeem, S., Abbas, N., Saleem, A., & Issakhov, A. (2020). Influence of Lorentz Force and Induced Magnetic Field Effects on Casson Micropolar Nanofluid Flow Over a Permeable Curved Stretching/Shrinking Surface Under the Stagnation Region. *Surfaces and Interfaces*, 21, 100766. https://doi.org/10.1016/j.surfin.2020.100766

Anwar, M., Shafie, S., Hayat, T., Shehzad, S., & Salleh, M. (2017). Numerical Study for MHD Stagnation-Point Flow of a Micropolar Nanofluid Towards a Stretching Sheet. *Journal of the Brazilian Society of Mechanical Sciences and Engineering*, 39, 89-100. https://doi.org/10.1007/S40430-016-0610-Y

Aparna, P., Murthy, J. R., & Nagaraju, G. (2018). Couple on a rotating permeable sphere in a couple stress fluid. *Ain shams engineering journal*, *9*(4), 665-673. https://doi.org/10.1016/j.asej.2016.03.012

Aparna, P., Nagaraju, G., & Kuruva, K. M. (2024). Analytical investigations of the hydrodynamic behavior of fluid with rotary oscillations permeable sphere in Jeffery fluid under magnetic field. *Multiscale and Multidisciplinary Modeling, Experiments and Design*, *8*(7), 302. HTTPS://DOI.ORG/10.1007/S41939-025-00895-Z

Aparna, P., Padmaja, P., Pothanna, N., & Murthy, J. R. (2022). Uniform flow of viscous fluid past a porous sphere saturated with micro polar fluid. *Biointerface Res. Appl. Chem.*, *13*(1), 69. https://doi.org/10.33263/BRIAC131.069

Aparna, P., Pothanna, N., & Ramana Murthy, J. V. (2018). Viscous fluid flow past a permeable cylinder. In *Numerical Heat Transfer and Fluid Flow: Select Proceedings of NHTFF 2018* (pp. 285-293). Singapore: Springer Singapore. https://link.springer.com/chapter/10.1007/978-981-13-1903-7_33

Aparna, P., Pothanna, N., Murthy, J. R., & Sreelatha, K. (2017). Flow generated by slow steady rotation of a permeable sphere in a micro-polar fluid. *Alexandria Engineering Journal*, *56*(4), 679-685. https://doi.org/10.1016/j.aej.2017.01.018

Avram, A., Avram, M., Volmer, M., Poenar, D. P., & Iliescu, C. Magnetic–Based Microfluidic Platform for Biomolecular Separation. *New Applications of Micro-and Nanotechnologies*, 9. http://www.ear.ro/

Awan, A., Akbar, A., Hamam, H., Gamaoun, F., Tag-ElDin, E., & Abdulrahman, A. (2022). Characterization of the Induced Magnetic Field on Third-Grade Micropolar Fluid Flow Across an Exponentially Stretched Sheet. *Frontiers in Physics*, 10, 964653. https://doi.org/10.3389/fphy.2022.964653

Baranwal, D. and Deshmukh, T. (2012). MR-fluid technology and its application - a review. International Journal of Emerging Technology and Advanced Engineering, 2(12):563–569. http://www.ijetae.com/

Danson, N., Jimrise, O., Jacob, K., Mark, O. (2025). Hydromagnetic Casson Nanofluid Flow Past a Wedge in a Porous Medium in the Presence of Induced Magnetic Field. American Journal of Applied Mathematics, 13(1), 30-56. https://doi.org/10.11648/j.ajam.20251301.13

Gerbeth, G., Dulikravich, G. S., and Pericleous, K. (2008). Computational electromagneto-hydro-dynamics (emhd). In 8th World Congress on Computational Mechanics (WCCM8), Venice, Italy.

Haverkort, J. and Peeters, T. (2009). Magnetohydrodynamics of insulating spheres. Magnetohydrodynamics, 45(1): 111–126. https://doi.org/10.22364/mhd.45.1.11

Hayat, T., Nawaz, M., & Hendi, A. (2011). Flow of Magnetohydrodynamic Micropolar Fluid Induced by Radially Stretching Sheets. Zeitschrift fu¨r Naturforschung A, 66, 5360. https://doi.org/10.1515/zna-2011-1-209

Jha, B. K. and Aina, B. (2016). Role of induced magnetic field on mhd natural convection flow in vertical microchannel formed by two electrically non-conducting infinite vertical parallel plates. Alexandria Engineering Journal, 55(3):2087– 2097. https://doi.org/10.1016/j.aej.2016.06.030

Kumar, A. and Singh, A. (2013). Unsteady mhd free convective flow past a semi-infinite vertical wall with induced magnetic field. Applied mathematics and computation, 222:462–471. https://doi.org/10.1016/j.amc.2013.07.044

Mahabaleshwar, U., Vishalakshi, A., & Hatami, M. (2022). MHD Micropolar Fluid Flow Over a Stretching/Shrinking Sheet with Dissipation of Energy and Stress Work Considering Mass Transpiration and Thermal Radiation. *International Communications in Heat and Mass Transfer*. https://doi.org/10.1016/j.icheatmasstransfer.2022.105966

Mustafa, B. T., Yaba, S. P., & Ismail, A. H. (2019). A review of the Effects of Magnetic Field on main blood cells: in vivo and in vitro experiments. *ZANCO Journal of Pure and Applied Sciences*, *31*(6), 40-50. https://zancojournals.su.edu.krd/index.php/JPAS

Patel, H., & Singh, R. (2019). Thermophoresis, Brownian Motion, and Non-Linear Thermal Radiation Effects on Mixed Convection MHD Micropolar Fluid Flow Due to Nonlinear Stretched Sheet in Porous Medium with Viscous Dissipation, Joule Heating and Convective Boundary Condition. *International Communications in Heat and Mass Transfer*. https://doi.org/10.1016/j.icheatmasstransfer.2019.05.007

Ramya, N., & Deivanayaki, M. (2024, January). Heat radiation on Casson nanofluid flow over an inclined stretching surface with heat and mass diffusions. In *International Conference on Recent Advancements in Materials Science and Technology* (pp. 355-367). Cham: Springer Nature Switzerland. https://doi.org/10.1007/978-3-031-69970-2_27.

Ramya, N., & Deivanayaki, M. (2025). Impact of Soret and Dufour Effects on Casson Nanofluid Flow in a Magnetic Field along with Heat and Mass Transfer. *Indian Journal of Science and Technology*, *18*(13), 1059-1070. https://doi.org/10.17485/IJST/v18i13.4028.

Ramya, N., Deivanayaki, M., & Pandurengan, S. (2025). Thermophoresis and Brownian motion effects on the Casson ternary hybrid nanofluid over a horizontal plate containing gyrotactic microorganisms. *Chemical Physics Impact*, *10*, 100887. https://doi.org/10.1016/j.chphi.2025.100887

Sheikholeslami, M. and Rokni, H. B. (2017). Nanofluid two-phase model analysis in existence of induced magnetic field. International Journal of Heat and Mass Transfer, 107:288–299. https://doi.org/10.1016/j.ijheatmasstransfer.2016.10.130

Singh, R. K., Singh, A. K., Sacheti, N. C., and Chandran, P. (2010). Hydromagnetic free

convection in the presence of induced magnetic field. Heat and Mass Transfer, 46:523–529. https:// DOI 10.1007/s00231-010-0594-6

Peer-review history:
The peer review history for this paper can be accessed here:
https://pr.sdiarticle5.com/review-history/141450